

# Consequences of Cysteine Mutations in Calcium-binding Epidermal Growth Factor Modules of Fibrillin-1\*

Received for publication, May 11, 2004  
Published, JBC Papers in Press, May 25, 2004, DOI 10.1074/jbc.M405239200

Tillman Vollbrandt‡, Kerstin Tiedemann‡, Ehab El-Hallous‡, Guoqing Lin‡,  
Jürgen Brinckmann‡, Harald John§, Boris Bätge¶, Holger Notbohm‡, and Dieter P. Reinhardt||

From the ‡Department of Medical Molecular Biology of the University of Lübeck, D-23538 Lübeck, Germany, §IPF PharmaCeuticals GmbH, D-30625 Hannover, Germany, and ¶Klinikum Neustadt, D-23730 Neustadt, Germany

**Mutations in fibrillin-1 lead to Marfan syndrome and some related genetic disorders. Many of the more than 600 mutations currently known in fibrillin-1 eliminate or introduce cysteine residues in epidermal growth factor-like modules. Here we report structural and functional consequences of three selected cysteine mutations (R627C, C750G, and C926R) in fibrillin-1. The mutations have been analyzed by means of recombinant polypeptides produced in mammalian expression systems. The mRNA levels for the mutation constructs were similar to wild-type levels. All three mutated polypeptides were secreted by embryonic kidney cells (293) into the culture medium. Purification was readily feasible for mutants R627C and C750G, but not for C926R, which restricted the availability of this mutant polypeptide to selected analyses. The overall folds of the mutant polypeptides were indistinguishable from the wild-type as judged by the ultrastructural shape, CD analysis, and reactivity with a specific antibody sensitive for intact disulfide bonds. Subtle structural changes caused by R627C and C750G, however, were monitored by proteolysis and heat denaturation experiments. These changes occurred in the vicinity of the mutations either as short range effects (R627C) or both short and long range effects (C750G). Enhanced proteolytic susceptibility was observed for R627C and C750G to a variety of proteases. These results expand and further strengthen the concept that proteolytic degradation of mutated fibrillin-1 might be an important potential mechanism in the pathogenesis of Marfan syndrome and other disorders caused by mutations in fibrillin-1.**

Fibrillins are major components of a class of 10–12-nm extracellular microfibrils, which occur either in association with elastin or in elastin-free bundles (1, 2). The highly homologous fibrillin family consists of three members, fibrillin-1, -2, and -3, which are encoded by different genes (2–7). Like many other extracellular glycoproteins, fibrillins are composed of individual modules in a mosaic fashion (Fig. 1A). Most of these modules are rich in cysteine residues, accounting for the high overall content of cysteine residues in fibrillins (12–13%). Mul-

tiply tandem arrays of epidermal growth factor-like (EGF)<sup>1</sup> domains constitute the majority of the fibrillin molecules. There are 46–47 EGF modules in each fibrillin, 42–43 of which are associated with calcium binding. Each EGF module contains six highly conserved cysteine residues, which form disulfide bonds in a 1–3, 2–4, 5–6 arrangement, generating an anti-parallel  $\beta$ -pleated sheet conformation (8, 9). It has been shown that calcium binding to calcium-binding EGF (cbEGF) modules in fibrillin-1 protects the molecules against proteolytic degradation by a variety of proteases (10) and that calcium plays a crucial role in stabilizing tandem repeats of cbEGF modules in fibrillin-1 (9, 11). Other prominent modules in fibrillins are 8-cysteine-containing structures typically referred to as 8-Cys/TB modules and hybrid modules. Both types of modules are exclusively found in fibrillins and latent transforming growth factor- $\beta$ -binding proteins (for a review, see Ref. 12).

Mutations in fibrillins lead to various connective tissue disorders such as the Marfan syndrome (MFS; MIM 154700) and some other related disorders of connective tissue commonly referred to as type-1 fibrillinopathies caused by mutations in the gene for fibrillin-1 (*FBN1*), and congenital contractural arachnodactyly (CCA; MIM 121050) caused by mutations in the gene for fibrillin-2 (*FBN2*) (for a review, see Ref. 13). Most of the known mutations in *FBN1* (95%) result in various forms of MFS (14). MFS is an autosomal dominant disorder of connective tissue with an estimated prevalence of about 1 in 5000 individuals (15). MFS is characterized by highly variable clinical manifestations including aortic dilation and dissection, ectopia lentis, dolichostenomelia, arachnodactyly, scoliosis, pectus deformities, and other musculoskeletal abnormalities (15).

A dominant negative model for the pathogenesis of MFS has been proposed in which the product of the mutant allele interferes with polymerization of fibrillin into microfibrils or destabilizes the microfibrils after incorporation, and the severity of the disease is dependent on the mutant protein level (16). In addition, other mechanisms must play a role, since some premature termination mutations that cause selective degradation of the mutant mRNA can result in severe disease (17–19). Independent of the involved mechanism, the common pathway of various types of mutations appears to involve a reduction in the amount of functional microfibrils in the extracellular matrix (20).

The majority of the more than 600 mutations in *FBN1* currently known are point mutations (72.4%); the rest are frame-

\* This work was supported by Deutsche Forschungsgemeinschaft Grants SFB 367-A1, Re1021/3-2, and Re1021/4-2. The costs of publication of this article were defrayed in part by the payment of page charges. This article must therefore be hereby marked "advertisement" in accordance with 18 U.S.C. Section 1734 solely to indicate this fact.

|| To whom correspondence should be addressed: Dept. of Medical Molecular Biology, University of Lübeck, Ratzeburger Allee 160, D-23538 Lübeck, Germany. Tel.: 49-451-500-4086; Fax: 49-451-500-3637; E-mail: reinhardt@mollbio.uni-luebeck.de.

<sup>1</sup> The abbreviations used are: EGF, epidermal growth factor-like module; cbEGF, calcium-binding epidermal growth factor-like module; 8-Cys/TB, 8-cysteine-containing modules; mAb, monoclonal antibody; MFS, Marfan syndrome; TBS, Tris-buffered saline; CCA, congenital contractural arachnodactyly.

shifts caused by deletions and insertions (16.1%) and splice site mutations (11.5%) (data set of the *FBN1* online data base (available on the World Wide Web at [www.umd.be](http://www.umd.be)) as of April 2004; see Ref. 14). Missense point mutations substituting (28.0%) or generating new (6.7%) cysteine residues represent the largest group, whereby the majority of cysteine-substituting (23.1%) or cysteine-generating (3.8%) mutations occur in cbEGF modules. Another prominent group (8%) are missense mutations that affect amino acid residues in cbEGF modules involved in calcium binding. For both groups, it is predicted that the mutations locally abolish or reduce calcium binding either directly by changing residues involved in calcium binding or indirectly by changing the structure of the mutated cbEGF module. It has been shown *in vitro* that a number of mutations affecting calcium binding residues render fibrillin-1 more susceptible to proteolysis, providing a potential mechanistic explanation for dominant negative effects (21–23). For some of these mutations, it has been shown that the enhanced susceptibility is caused by subtle structural changes in the region of the mutation (22). For the much larger group of cysteine mutations, however, very little information is available on their structural and functional consequences. Based on quantitative pulse-chase analyses of a number of cysteine mutations, normal synthesis and stability were observed for the majority of mutations analyzed accompanied with delayed secretion in about 55% (24). In another study, two cysteine mutations studied in a recombinant system were retained and accumulated in the cells (25). Enhanced protease susceptibility induced by a cysteine mutation have been shown in another study (26).

Here we demonstrate that typical cysteine mutations in cbEGF modules, which result in the classical form of Marfan syndrome, render recombinantly expressed polypeptides susceptible to proteolysis. Structural analyses reveal minor changes introduced by the mutations. These results extend and strengthen the concept that enhanced proteolytic degradation of mutated fibrillin-1 may be the causative mechanism for at least certain groups of mutations leading to type-1 fibrillinopathies.

#### EXPERIMENTAL PROCEDURES

**Expression Constructs**—The construction of an episomal plasmid pCEPSP-rF45 to express wild-type human fibrillin-1 fragment rF45 (Asp<sup>451</sup>-Lys<sup>1027</sup>) as well as the cloning plasmid pBS-rF45 was described in detail previously (22). To introduce the mutation C1879T leading to amino acid substitution R627C (27), site-directed mutagenesis was performed with plasmid pBS-rF45 and complementary primer pairs 5'-GATCTGCATGAATGGGTTGTT GCGTCAACACTG-3' and 5'-CAGTGTGACGCAACCCATTCATGCAGATC-3' using the QuikChange™ procedure as instructed by the supplier (Stratagene). Mutations in the oligonucleotides are in boldface type and underlined. The resulting plasmid was restricted with NheI-NotI, and the 1745-bp fragment was subcloned into the NheI-NotI-restricted pCEPSP-rF45, resulting in pCEPSP-rF45-C1879T. To introduce the mutation T2248G, leading to amino acid substitution C750G (27), an analogous procedure was employed using primer pairs 5'-GGGACCTATAAATGTATAG-GCAATTCAGGATATGAAGTGG-3' and 5'-CCACTTCATATCCT-GAATTGCCATATACATTTATAGGTTCCC-3'. To produce the mutation T2776C resulting in amino acid substitution C926R (28), template HFBN23 was used to amplify a 346-bp fragment with sense primer 5'-CCTTGCATTAATGGAGTCTGC-3' and antisense primer 5'-TAGTGTAAACAGCAGGCCATTTTTACACACTCC-3' by polymerase chain reaction. A 267 bp BamHI-HpaI fragment was excised from the product and subcloned into the BamHI-HpaI-restricted pBS-rF45 plasmid. A 1745-bp NheI-NotI fragment was then subcloned into NheI-NotI-restricted pCEPSP-rF45, resulting in pCEPSP-rF45-T2776C. Correct insertions of all mutations as well as the absence of new mutations introduced by DNA amplification were verified by DNA sequencing. All mutation constructs code for a protein with the sequence Ala-Pro-Leu-Ala-Asp<sup>451</sup>-Lys<sup>1027</sup> including the individual mutation and without an additional histidine tag.

The Flp-In system was used to generate stable recombinant cell

clones with exactly one copy of the expression plasmid incorporated at a predefined locus of the cellular genome (Invitrogen). All mutation constructs in the pCEPSP plasmids were restricted with NheI-NotI, and the 1745-bp fragments were subcloned into NheI-NotI-restricted pcDNA5-FRT plasmid (Invitrogen), which had been modified by adding the sequence encoding the BM40 signal peptide. The sequences of the proteins expressed were identical to what is described above for the pCEPSP expression plasmids.

To facilitate epitope mapping, several new expression plasmids for fragments of human fibrillin-1 have been generated. All of the following expression constructs are designed with a His<sub>6</sub> tag at the C-terminal end to facilitate protein purification. To assemble an expression plasmid coding for Ser<sup>19</sup>-Gly<sup>714</sup> of human fibrillin-1, plasmid pDNSP-rF16 (29) was cut with EcoRI-NotI, and the 7516-bp fragment was religated using two complementary oligonucleotides 5'-AATTCAGCGGAATATCAGGCACTCTGCAGCAGTGGGCATCACCATCACCACTACTAATAGTGC-3' and 5'-GGCCGCACTATTAGTGTGATGGTGTGATGTGCCACTGCTGCAGAGTGCCTGATATTCGCGTG-3' as linkers. The resulting plasmid pDNSP-rF1F codes for a recombinant polypeptide (rF1F) with the sequence Ala-Pro-Leu-Ala-Ser<sup>19</sup>-Gly<sup>714</sup>-His<sub>6</sub>. An expression plasmid coding for Asp<sup>613</sup>-Leu<sup>951</sup> was generated by amplification of template HFBN23–29 (30) with primers 5'-CGTAGCTAGCAGACATTAACGAGTGTGAAACCC-3' and 5'-ACCGCTCGAGCTATTAGTGTGATGGTGTGATGAAGACAGATCCTTCTGTGGC-3'. The product was restricted with NheI-XhoI (1048 bp) and subcloned into pDNSP-rF16 (29) restricted with the same enzymes. The resulting plasmid codes for a recombinant protein (rF51) with the sequence Ala-Pro-Leu-Ala-Asp<sup>613</sup>-Leu<sup>951</sup>-His<sub>6</sub>. To prepare an expression plasmid coding for Asp<sup>723</sup>-Leu<sup>951</sup>, HFBN23–29 (30) was amplified with primers 5'-CGTAGCTAGCTGATATAAATGAATGTGCACTAGATCC-3' and 5'-ACCGCTCGAGCTATTAGTGTGATGGTGTGATGGTGTGATGAAGACAGATCCTTCTGTGGC-3'. The resulting product was cut with NheI-XhoI (730 bp) and subcloned into the NheI-XhoI-restricted pcDNA5-FRT plasmid (Invitrogen) including a sequence for the BM40 signal peptide. The resulting expression plasmid codes for the recombinant polypeptide rF1A with the sequence Ala-Pro-Leu-Ala-Asp<sup>723</sup>-Leu<sup>951</sup>-His<sub>6</sub>. To assemble an expression plasmid coding for Asp<sup>952</sup>-Lys<sup>1027</sup>, template pCEPSP-rF18 (30) was amplified by polymerase chain reaction with primers 5'-CGTAGCTAGCCGATATCCGCTGGAAACCTGC-3' and 5'-ATAGTTTACGCGCCGCTAGTGTGATGGTGTGATGGTGTGATTTGAGAAAGGCTTTCCATTTG-3'. A 256-bp fragment (NheI-NotI) was cut from the product and subcloned into the NheI-NotI-restricted pCEPSP-rF18, resulting in pCEPSP-rF35. This expression plasmid codes for recombinant polypeptide rF35 with the sequence Ala-Pro-Leu-Ala-Asp<sup>952</sup>-Lys<sup>1027</sup>-His<sub>6</sub>. The relative position of all expressed polypeptides in comparison with full-length fibrillin-1 is shown in Fig. 1A.

**Transfection of Cells and Culture Conditions**—293-EBNA cells (Invitrogen) were used to generate episomal recombinant cell clones with the pCEPSP plasmids. Flp-In-293 cells (Invitrogen) were used to generate stable recombinant cell clones with the pcDNA5-FRT plasmids, and 293 cells (American Type Culture Collection) were used for the production of stable clones with the pDNSP-based plasmids. All cell types were grown in Dulbecco's modified Eagle's medium supplemented with 2 mM glutamine, 100 units/ml penicillin, 100 µg/ml streptomycin, and 10% fetal calf serum in a 5% CO<sub>2</sub> atmosphere at 37 °C. For 293-EBNA and 293 cells, calcium phosphate transfection was performed as described in detail (31). For Flp-In-293 cells, cotransfection with a plasmid encoding the Flp recombinase (pOG44) was performed as instructed by the supplier (Invitrogen). Selection of recombinant clones was started after 24 h with 0.25 mg/ml hygromycin (293-EBNA, Flp-In-293) or 0.25 mg/ml G418 (293). Single colonies resistant to the antibiotics were picked and propagated. Positive clones were identified by analysis of conditioned medium by Western blotting and SDS-gel electrophoresis using standard protocols.

**mRNA Synthesis and Secretion of Recombinant Proteins**—Nontransfected and transfected Flp-In-293 cell clones were grown to confluence in 75-cm<sup>2</sup> flasks and used for RNA purification and secretion analysis. After isolation of total RNA with Trizol following the supplier's instructions (Invitrogen), the mRNA was reverse transcribed into cDNA with Superscript II and oligo(dT) primer according to the manufacturer's protocol (Invitrogen). Polymerase chain reaction was performed using *Taq* polymerase (Roche Applied Science) and primer pair 5'-AAGTGTGTCAGTGTCCCAGTGG-3' and 5'-TAGAAGGCACAGTCGAGGC-3', which produced a 350-bp fragment specific for the rF45 constructs. A standard control (glyceraldehyde-3-phosphate dehydrogenase) was included, which resulted in a 1173-bp DNA fragment. The intensity of the DNA fragments was visualized by standard agarose gel electrophoresis and ethidium bromide staining. The conditions for the

DNA amplifications (rF45 constructs and control) were optimized for quantification with respect to the cycle number and the amount of cDNA used as template. For this goal, the intensities of the stained DNA bands were correlated with a wide range of cycle numbers and the amount of cDNA used in the amplification procedure. The final parameters for quantification were chosen from linear ranges and were 0.5  $\mu$ l of template cDNA solution for both reactions, 26 cycles for the recombinant constructs, and 22 cycles for the control.

To test the secretion of the recombinant polypeptides, confluent cell layers were washed twice with phosphate-buffered saline and incubated with 10 ml of serum-free Dulbecco's modified Eagle's medium, which was harvested after 48 h. Equal amounts (1 ml) of secreted proteins, precipitated from the serum-free medium with 10% (w/v) trichloroacetic acid, were analyzed by standard Western blotting techniques using monoclonal antibody (mAb) 201 (~4  $\mu$ g/ml), which is specific for authentic fibrillin-1 and only reacts with nonreduced material (1, 22).

**Production and Purification of Recombinant Polypeptides**—For large scale production of rF45-wt, rF45-R627C, rF45-C750G, rF45-C926R, and the histidine tag-containing recombinant polypeptides rF35, rF51, rF1A, and rF1F, cells were grown in triple layer flasks (500 cm<sup>2</sup>; Nalge Nunc International) to confluence, washed twice with 20 mM HEPES, 150 mM NaCl, pH 7.4, or alternatively with serum-free Dulbecco's modified Eagle's medium and incubated with 60–70 ml of serum-free Dulbecco's modified Eagle's medium for 48 h. The conditioned medium was centrifuged for 15 min at 4 °C (5000  $\times$  g) to remove cells, supplemented with phenylmethylsulfonyl fluoride (Fluka) to a final concentration of 0.1 mM, and frozen at –20 °C. About 2–3 liters of serum-free medium were collected and concentrated by ultrafiltration (10–30-kDa cut-off) to 40–50 ml. For the recombinant polypeptides without a histidine tag (rF45 wild-type and mutation constructs), the concentrated medium was dialyzed against 20 mM Tris-HCl, pH 8.6. The dialyzed medium was passed over an anion exchange column (1 ml of HiTrap Q; Amersham Biosciences) equilibrated in the same buffer, and bound proteins were eluted with a gradient of 25 mM NaCl/ml (0–400 mM NaCl total). Fractions containing the recombinant polypeptides were pooled and concentrated by ultrafiltration (10-kDa cut-off) to ~1.5 ml. Fractions of ~0.5 ml were passed over a Superose 12 gel filtration column (24 ml; Amersham Biosciences) equilibrated in 50 mM Tris-HCl, pH 7.4, 150 mM NaCl (TBS). Fractions containing the protein of interest were pooled and stored at –80 °C. Purification of recombinant polypeptides with a His<sub>6</sub> tag (rF35, rF51, rF1A, and rF1F) was performed by chelating chromatography as described in detail previously for other recombinant polypeptides with minor modifications (32). Assessment of the purity and visualization of the purified material was performed by standard SDS gel electrophoresis and Coomassie Blue staining.

**Epitope Mapping**—Overlapping recombinant fragments of the N-terminal part of fibrillin-1 were used to localize the epitope of mAb 201 by standard Western blotting as described in detail (33). The purified recombinant fragments (5  $\mu$ g each) were subjected to SDS-gel electrophoresis under nonreducing conditions, transferred to nitrocellulose membrane, and incubated with ~4  $\mu$ g/ml mAb 201. To correlate bands recognized by mAb 201 with the position of the purified proteins, a control was included with Coomassie Blue-stained purified polypeptides after SDS gel electrophoresis under reducing and nonreducing conditions.

**Degradation Experiments and N-terminal Sequence Analysis**—Recombinant polypeptides rF45-wt, rF45-R627C, and rF45-C750G (1.0 mg/ml in TBS) were supplemented with 5 mM CaCl<sub>2</sub> and incubated for 10 min at room temperature. After removal of a control, enzymes were added at a concentration of 1:20 (w/w) for plasmin (EC 3.4.21.7; Roche Applied Science) or 1:100 (w/w) for trypsin (EC 3.4.21.4; Sigma) treated with tosylphenylalanyl chloromethyl ketone and  $\alpha$ -chymotrypsin (EC 3.4.21.1; Sigma) treated with N<sup>α</sup>-p-tosyl-L-lysine chloromethyl ketone for incubation periods of 60 min (plasmin) or 10 min (trypsin and chymotrypsin). The reaction was stopped by adding 2-fold concentrated reducing SDS sample buffer to equal aliquots of the samples and heating at 95 °C for 3 min. Degradation products were separated by SDS gel electrophoresis (7.5–12% gradient gels) and visualized by Coomassie Blue staining.

For N-terminal sequence analysis, the degradation products were blotted on polyvinylidene difluoride membrane (Immobilon-P (Millipore) or Pro Blott (Applied Biosystems)), stained with Coomassie Blue, excised, and analyzed on a protein sequencer (Applied Biosystems model 494).

**Circular Dichroism Spectroscopy**—The purified recombinant polypeptides rF45-wt, rF45-R627C, and rF45-C750G (0.5 mg/ml in TBS) were analyzed either in the presence of 5 mM CaCl<sub>2</sub> or 0.25 mM EDTA from 200 to 260 nm in a quartz cuvette at 20 °C on a Jasco J-715

instrument. Heat denaturation of the purified recombinant polypeptides was determined by measuring the circular dichroism at 220 nm at increasing temperatures (20–100 °C in steps of 0.4 °C/min). The signal at 20 °C was set to 0% denaturation, and the signal at 100 °C was set to 100% denaturation.

**Low Angle Rotary Shadowing Electron Microscopy**—Purified polypeptides rF45-wt, rF45-R627C, rF45-C750G, and rF45-C926R (~0.25 mg/ml) were supplemented with 5 mM CaCl<sub>2</sub> and dialyzed against H<sub>2</sub>O. The samples were mixed with equal volumes of glycerol to a final concentration of 50% (v/v) glycerol, sprayed onto freshly cleaved mica, and dried under vacuum (Edwards Auto 306). Rotary shadowing was performed as described in detail previously (32). Replicates were examined at 100 kV in a transmission electron microscope (Zeiss TEM 109).

## RESULTS

In this study, we have investigated structural and functional consequences of cysteine mutations in fibrillin-1, leading to the classical form of MFS. Missense mutations substituting or eliminating cysteine residues in cbEGF modules represent the largest group of mutations in fibrillin-1 (see Introduction and Ref. 14). The mutations in the FBN1 gene analyzed in this study were C1879T and T2248G, resulting in an additional cysteine residue (R627C) in cbEGF module 6 or a cysteine substitution at the C5 position of cbEGF module 7 (C750G), respectively (27). The third mutation analyzed was T2776C, leading to a cysteine substitution at the C3 position of cbEGF module 10 (C926R) (28). The mutations were introduced by site-directed mutagenesis into the expression vector for the previously described fibrillin-1 wild-type construct rF45-wt, spanning the fourth generic non-calcium-binding EGF-like module to the third 8-Cys/TB module (Fig. 1A) (22). The relative position of the cysteine mutations within a typical cbEGF module is shown in Fig. 1B.

In order to analyze and compare mRNA expression and protein secretion from cells, stable expression clones were generated with the Flp-In system (Invitrogen). With this system, exactly one copy of the expression plasmid is incorporated into a predefined locus in the genome of the cells, eliminating differences of the copy number and the locus between different recombinant cell clones. Analysis of the mRNA by polymerase chain reaction after reverse transcription into cDNA demonstrated that all recombinant clones expressed the mutant mRNA at similar levels as compared with the wild type (Fig. 2A). Control analyses of mRNA isolated from nontransfected Flp-In-293 cells did not show any detectable PCR product (not shown).

Analyses by Western blotting with a specific monoclonal antibody (mAb 201) of conditioned nonreduced medium demonstrated that all three mutated polypeptides were secreted into the culture medium, whereby the amounts detected varied between experiments in particular for mutant C926R (Fig. 2B). These results show that the cysteine mutations analyzed do not prevent secretion of the recombinant mutants in the epithelium-derived cell line 293, which abundantly produce endogenous fibrillin-1 and -2. However, it is possible that secretion patterns in mesenchymal cells such as fibroblasts are different. For rF45-R627C and rF45-C750G, the molecular mass of the major reactive band (~63 kDa) corresponded well with the wild-type construct (Fig. 2B, lanes 1–3). In addition, faint bands corresponding to the positions of dimers have been observed. The mutated polypeptide rF45-C926R often showed a somewhat smaller molecular mass of ~58 kDa and higher molecular mass aggregates probably representing dimers, trimers, and tetramers (Fig. 2B, lane 4). These results indicate that rF45-C926R is proteolytically processed in the close vicinity of the mutation, which is situated close to the end of the molecule (Fig. 1A). All three mutation constructs were detected with mAb 201, an antibody that depends on intact disulfide

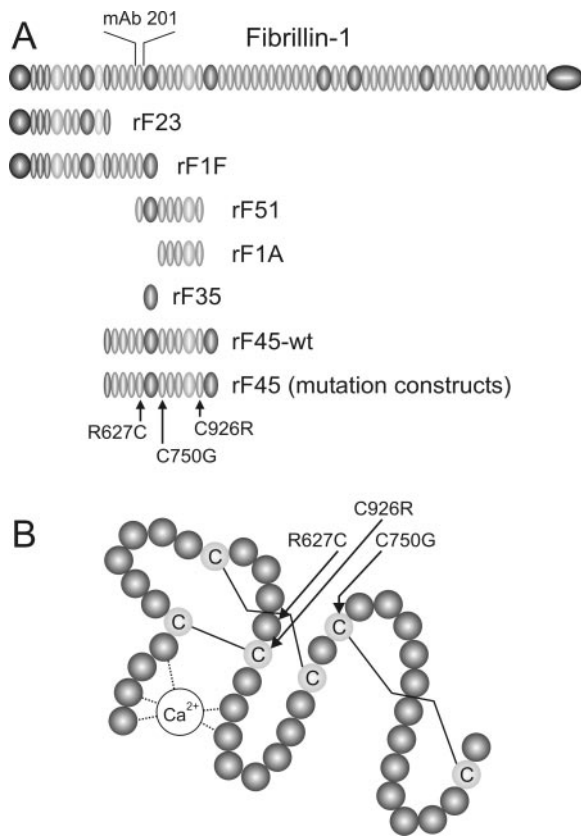


**FIG. 1. Schematic drawing of recombinantly expressed polypeptides and a cbEGF module.** *A*, the relative positions and sizes of the recombinant polypeptides used in this study are shown in comparison with the full-length human fibrillin-1. rF23 and rF45-wt have been produced previously (22, 34), whereas the remaining polypeptides have been produced in this study. The positions of the mutations introduced (R627C, C750G, and C926R) into the rF45-wt polypeptide and the epitope for mAb 201 are indicated. *B*, schematic drawing of a cbEGF module. Each circle represents one amino acid residue. Conserved cysteine residues are labeled *C*, and disulfide bonds are indicated by black lines. The relative positions of cysteine mutations R627C, C750G, and C926R are highlighted by arrows.

bonds (22). In order to correlate the mutated sites with the epitope for mAb 201, we intended to exactly map the epitope for mAb 201. For this analysis, various new overlapping recombinant fibrillin-1 polypeptides (rF35, rF51, rF1A, and rF1F) have been recombinantly produced in 293 cells and purified to homogeneity (Figs. 1A and 3A). Molecular properties of these new recombinant polypeptides are summarized in Table I. Using these recombinant polypeptides together with previously described recombinant polypeptides rF23 and rF45 (Fig. 1A) (22, 34) in Western blot analyses with mAb 201 resulted in the epitope mapping to cbEGF module 6 (Fig. 3B). The mAb 201 epitope is schematically shown in Fig. 1A. Since the mutations R627C and C750G are situated in or very close to the mAb 201 epitope in cbEGF modules 6 and 7 (see Fig. 1A), we conclude that these mutations do not perturb the overall disulfide bonding pattern in this region.

Although advantageous for the quantification of mRNA and secretion studies, the recombinant Flp-In mutation clones could not be used for large scale recombinant protein production, since the protein expression level was relatively low (<100 ng of protein/ml/day), and, in addition, the cells detached from the culture vessels after a few days of culture time. Therefore, stable recombinant episomal cell clones were generated in 293-EBNA cells. Purification of the recombinant clones by anion exchange chromatography followed by gel filtration typically yielded about 1 mg of protein/liter of conditioned medium for

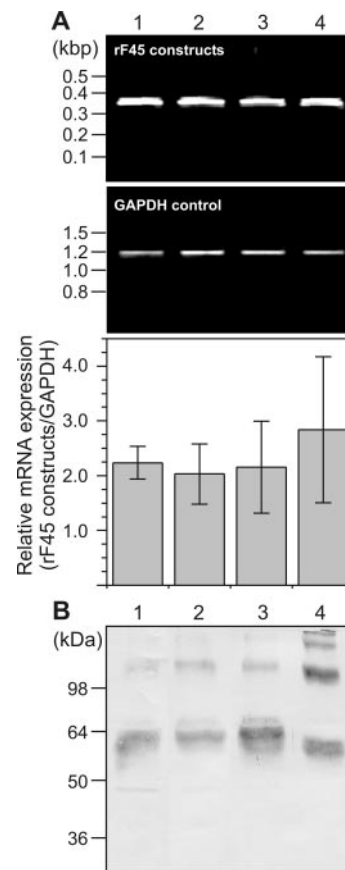


**FIG. 2. mRNA synthesis and protein secretion of recombinant cell clones.** Recombinant Flp-In-293 clones transfected with pcDNA5-FRT expression plasmids for rF45-wt (1), rF45-R627C (2), rF45-C750G (3), and rF45-C926R (4) were used for the analyses. *A*, mRNA of each construct (*upper panel*, rF45 constructs) or glyceraldehyde-3-phosphate dehydrogenase as a control (*middle panel*, GAPDH control) was transcribed into cDNA, amplified by polymerase chain reaction, and visualized by ethidium bromide staining after gel electrophoresis. The amount of total RNA used (1  $\mu$ g) was identical for each sample. Representative bands are shown. The relative mRNA expression (relative mRNA expression (rF45 constructs/GAPDH)) was determined by densitometric analyses of electrophoretic bands. The plotted data represent the average of six PCR amplifications. The bars represent S.D. values. Analysis of the data using an unpaired Student's *t* test with assumed equal variances revealed no statistically significant differences (two-tailed *p* values > 0.3). *B*, the secretion of recombinant polypeptides from cells were tested by Western blotting. Equal aliquots (1 ml) of conditioned medium (48 h) were analyzed under nonreducing conditions with mAb 201, which is specific for human fibrillin-1 and requires intact disulfide bonds. Positions of reduced marker proteins are indicated in kDa.

rF45-wt, rF45-R627C, and rF45-C750G. Although these polypeptides differ only in one amino acid residue in comparison with rF45-C926R, purification of the latter polypeptide consistently proved to be very difficult and inefficient, yielding at least 10-fold lower amounts in the range of 100  $\mu$ g of protein/liter of conditioned medium. The purification of rF45-C926R could not be improved using a variety of other purification methods. Due to this low yield, only selected experiments could be performed with purified rF45-C926R.

Electron microscopy after rotary shadowing of the mutated polypeptides showed frequently long extended molecules with some bends and kinks (Fig. 4A). Occasionally some curled molecules have been observed. The extended shape of the mutated polypeptides is very similar to the shape of the wild-type polypeptide, which has been analyzed in a previous study (22). This property is a strong indicator that the overall fold of the polypeptides is correct and has not been grossly affected by the mutations, since the extended shape depends on calcium bind-

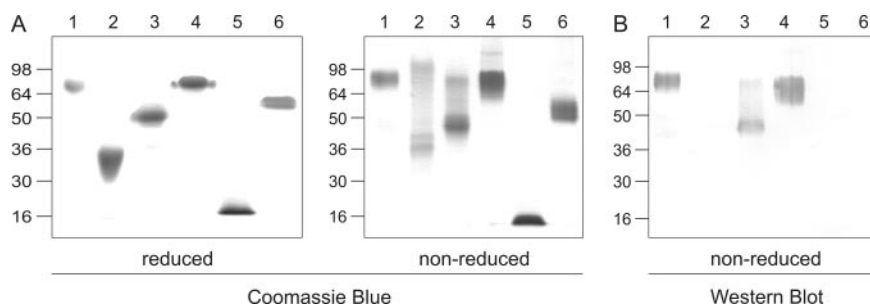


FIG. 3. **Purity of recombinant proteins and epitope mapping of mAb 201.** The recombinant polypeptides rF1F (1), rF1A (2), rF51 (3), rF45-wt (4), rF35 (5), and rF23 (6), shown schematically in Fig. 1A, have been analyzed by SDS gel electrophoresis under reducing (left panel) and nonreducing (right panel) conditions (A) and by Western blotting with mAb 201 under nonreducing conditions (B). Positions of reduced marker proteins are indicated in kDa.

TABLE I

Molecular masses of new recombinant polypeptides determined by SDS-gel electrophoresis

The recombinant polypeptides analyzed are schematically shown in Fig. 1A.

Recombinant polypeptide	Molecular mass	
	Reduced	Nonreduced
	<i>kDa</i>	
rF35	18	16
rF51	53	48
rF1A	31	37
rF1F	77	77

ing and correct disulfide bonds. Further analysis demonstrated for rF45-R627C a length of  $28.7 \pm 2.8$  nm ( $n = 26$ ) and for rF45-C750G a length of  $29.0 \pm 3.7$  nm ( $n = 23$ ) (Fig. 4B). These results correspond well with length measurements of rF45-wt ( $27.9 \pm 1.8$  nm) demonstrated previously (22). The number of well resolved particles obtained for rF45-C926R was not sufficient for statistical analysis.

The secondary structure of mutated polypeptides were analyzed by far-UV circular dichroism spectroscopy. The spectrum obtained for rF45-wt was very similar to the spectra for rF45-R627C and rF45-C750G with minima at 208 nm between  $\Theta_{MRW} = -5901$  and  $-6764$  for the calcium-loaded form and  $\Theta_{MRW} = -7277$  and  $-7677$  for the calcium-free form (Fig. 5A). The results are typical for fibrillin fragments containing large amounts of  $\beta$ -structures (22). The data indicate very similar overall secondary structures of the mutated and the wild-type polypeptides in the calcium-free as well as in the calcium-loaded form. Thermal denaturation profiles of the recombinant polypeptides monitored by circular dichroism at 220 nm, however, showed differences between wild-type and mutated polypeptides (Fig. 5B). rF45-wt showed a steep denaturation profile at temperatures between 60 and 90 °C with 50% denaturation at 78 °C. This is in good correlation with the observation that both fibrillin-1 and fibrillin-2 are very stable proteins (32). Both rF45-R627C and rF45-C750G showed much more shallow denaturation profiles spanning the region between 20 and 100 °C (Fig. 5B). In summary, the analysis by circular dichroism suggests no major structural changes rather than minor structural changes caused by the mutations.

The recombinant polypeptides were analyzed for their susceptibility to a variety of proteases such as trypsin, chymotrypsin, and plasmin. As shown previously, the control polypeptide rF45-wt preincubated with 5 mM calcium was virtually resistant to proteolytic cleavage by all three proteases (Fig. 6, top panel) (22). The mutated polypeptides rF45-R627C and rF45-C750G were in general significantly more susceptible to proteolytic cleavage (Fig. 6). rF45-R627C was sensitive to treatment with chymotrypsin and trypsin but not with plasmin (Fig. 6, middle panel). With both proteases, cleavage products of

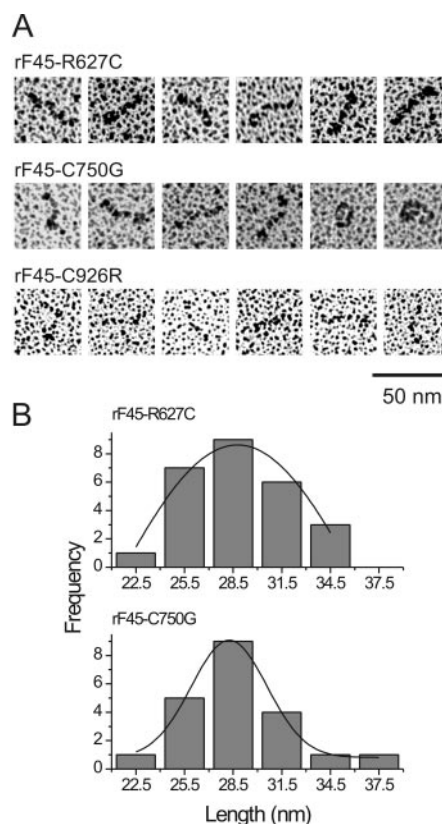
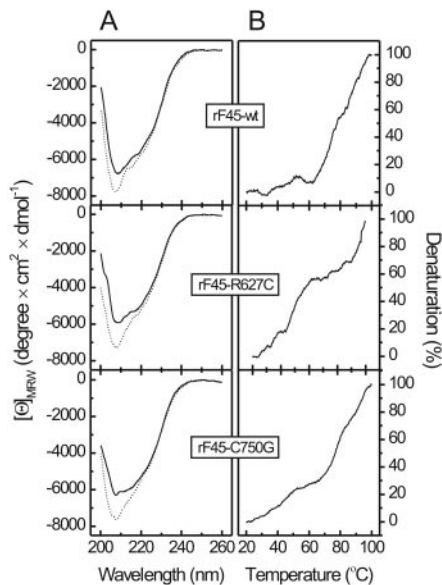


FIG. 4. **Shape and length of mutated polypeptides.** A, shown are electron microscopic images after rotary shadowing. Note that for rF45-C926R, only a few (and, in addition, not particularly well resolved) particles were found in the preparation. B, histogram of the measured lengths of rF45-R627C and rF45-C750G. Measurements are plotted as numbers of measurements in 3-nm windows (bars). Gaussian curves are shown for each measurement (curves).

about 25 and 50 kDa have been observed. rF45-C750G showed degradation products with all three proteases with major degradation fragments of about 40 and 45 kDa (Fig. 6, bottom panel). In the presence of 5 mM EDTA, the calcium-free forms of the wild-type as well as the mutated polypeptides showed significantly more degradation as compared with the calcium-loaded form (data not shown). N-terminal sequence analyses of proteolytic fragments found after protease incubation of rF45-R627C and rF45-C750G, which were protected in rF45-wt, are listed in Table II. For rF45-R627C, chymotrypsin detected a sensitive site at position 648, whereas trypsin cleaved at position 651. Both cleavage sites are situated relatively close to the mutated site in cbEGF module 6. For rF45-C750G, chymotrypsin cleaved at positions 755, 772, and 773, trypsin at positions 744 and 783, and plasmin at position 748. These sensitive sites



**FIG. 5. Far-UV circular dichroism spectra and heat denaturation of wild type and mutated polypeptides.** A, far UV circular dichroism measurements were performed either in the presence of 5 mM  $\text{CaCl}_2$  (solid lines) or in the presence of 0.25 mM EDTA (dotted lines) at 20 °C with 0.5 mg/ml recombinant polypeptides. Measurements at wavelengths below 200 nm are not shown due to strong absorption of the buffer. The residue ellipticity  $[\theta]_{\text{MRW}}$  is plotted as a function of wavelength. B, heat denaturation of recombinant polypeptides (0.5 mg/ml) was performed by incubation with increasing (0.4 °C/min) temperatures as indicated and monitored by measuring the far UV circular dichroism at 220 nm. The signal at 20 °C was set to 0% denaturation, and the signal at 100 °C was set to 100% denaturation.

are located close to the mutated site in cbEGF module 7 as well as in the C-terminally located cbEGF module 8. A schematic overview of all sensitive cleavage sites found in the mutated polypeptides is shown in Fig. 7.

#### DISCUSSION

More than 600 mutations in fibrillin-1 are recorded, which lead to MFS and some other related disorders (online *FBNI* mutation data base; see Ref. 14). The mutations are spread over the entire gene and thus over the entire fibrillin-1 protein. Genotype-clinical phenotype correlations have only been found for some mutations in a central portion of fibrillin-1, resulting in the severe neonatal Marfan syndrome (for a review, see Ref. 35). The consequences of most mutations on the biochemical phenotype of the fibrillin-1 protein are largely obscure. Here, we have analyzed the structural and functional consequences of three cysteine mutations in cbEGF modules, which represent the largest group of missense point mutations in fibrillin-1.

In order to analyze these consequences on the protein level, recombinant mammalian systems have been employed to produce protein fragments containing the mutations. Fragments of fibrillin-1 are more suitable for these studies, since recombinant full-length fibrillin-1 tends to aggregate, preventing a variety of analyses (32). We decided to analyze selected examples of a group of mutations that occur with high frequency (14). One of the cysteine-replacing mutations (C750G) affects the C5 position (4.2% of all mutations) in cbEGF module 7 and is therefore predicted to prevent formation of the C5–C6 disulfide bond. The second cysteine-replacing mutation (C926R) alters the position C3 (4.8% of all mutations) in cbEGF module 10 and is predicted to prevent proper formation of the C1–C3 disulfide bond. The third mutation analyzed in this study (R627C) introduces an additional cysteine residue directly preceding the cysteine in the C3 position of cbEGF module 6. This

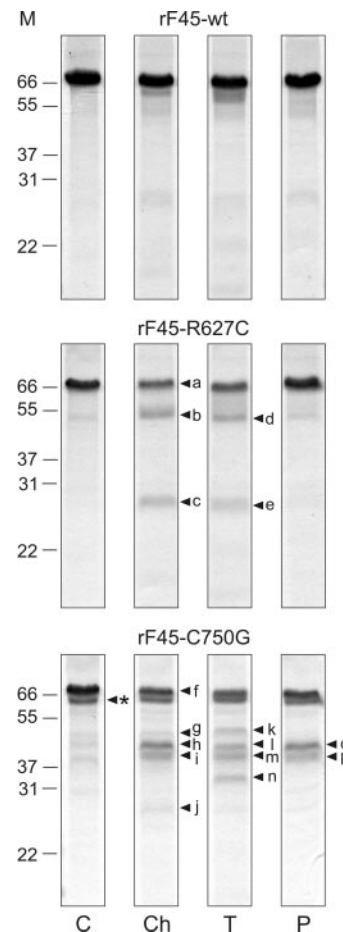


**FIG. 6. Degradation of recombinant polypeptides by various proteases.** Recombinant polypeptides rF45-wt, rF45-R627C, and rF45-C750G, preincubated with 5 mM calcium, were treated as specified under “Experimental Procedures” with chymotrypsin (*Ch*) for 10 min, with trypsin (*T*) for 10 min, and with plasmin (*P*) for 60 min and analyzed by SDS gel electrophoresis and Coomassie Blue staining. Controls (*C*) were not treated with proteases. The positions of reduced marker proteins are indicated in kDa (*M*). Proteolytic fragments of the mutated polypeptides that were not present or were less present in the rF45-wt (arrowheads and lowercase letters) have been further analyzed in parallel experiments by N-terminal sequencing. The results are summarized in Table II and in Fig. 7. The band marked with an asterisk represents a nonrelevant protein (bovine serum albumin).

mutation possibly interferes with formation of the C1–C3 or, alternatively, with the C2–C4 disulfide bond.

The Flp-In expression system used in this study is designed to incorporate exactly one copy of the expression plasmid at a fixed locus into the host genome (Invitrogen). In this system, the mRNA levels of all three recombinant mutation cell clones were comparable with the recombinant wild-type cell clone. The mutated proteins were synthesized and secreted into the culture medium as demonstrated by Western blot analyses of the conditioned medium. Large scale production of recombinant protein, however, was not feasible with the Flp-In recombinant cell clones, since the protein expression level was relatively low. Using an episomal expression system, constructs rF45-R627C and rF45-C750G could be produced in sufficiently large amounts, whereas it was not feasible to obtain sufficient amounts of rF45-C926R. One potential explanation is that rF45-C926R becomes degraded during the purification process. Due to the low yields of rF45-C926R, it could be only used in selected experiments.

In this study, we present for the first time structural consequences of cysteine mutations on the fibrillin-1 molecule. We have previously shown that the epitope of mAb 201 depends on

TABLE II  
Degradation products of mutant polypeptides

Degraded protein fragments indicated in Fig. 6 (code) were analyzed by N-terminal sequencing. X indicates residues that could not be unambiguously identified.

Protease	Code	N-terminal sequence	Position
rF45-R627C			
Chymotrypsin	a	APLADYXQLV	N terminus
	b	DGRVXVDTHM	648
	c	APLADYXQLV	N terminus
Trypsin	d	VXVXTXMR	651
	e	APLAXYXQ	N terminus
rF45-C750G			
Chymotrypsin	f	XPLADYX	N terminus
	g	APLADYXQLV	N terminus
	h	EVDSTXKXXVDI	755
	i	NSLLXDNXQ	772
Trypsin	j	SLLXDNGQ	773
	k	APLADYXQLV	N terminus
	l	APLAXYXQ	N terminus
		XTPGXFXV	783
		GTYKXIGN	744
		NTPGXFXV	783
Plasmin	n	APLAXYXQ	N terminus
	o	APLAXYXQ	N terminus
	p	XIGNSGYEV	748

intact disulfide bonds (22). Here, we have mapped the mAb 201 epitope to cbEGF module 6, providing the basis to conclude that introduction of a new cysteine (R627C) in cbEGF module 6 does not perturb the overall disulfide-bonding pattern. Electron microscopy after rotary shadowing demonstrated for all three mutated polypeptides that the overall threadlike structure, typical for fibrillin-1, was not significantly altered as compared with the wild-type polypeptide. This conclusion was further substantiated by analysis of the secondary structures by circular dichroism spectroscopy. Profiles typical for proteins containing tandem repeats of cbEGF modules with large amounts of  $\beta$  structures were obtained for rF45-R627C and rF45-C750G (22, 36). These profiles were very similar to the profiles obtained from the wild-type polypeptide in the calcium-loaded as well as in the calcium-free forms. However, heat denaturation profiles demonstrated a less stable conformation for the mutant rF45-R627C and rF45-C750G as compared with the wild-type polypeptide. These data indicated subtle structural changes in the mutated polypeptides, which were sufficient to nucleate thermal denaturation processes. Subtle structural changes caused by mutations leading to MFS have also been observed for some noncysteine mutations (22, 37).

These data were confirmed and substantiated by protease digestion studies. Both polypeptides, rF45-R627C and rF45-C750G, were more sensitive to proteolytic degradation by a variety of proteases, demonstrating that the mutations altered the structure so that cryptic sites became accessible to proteolytic attacks (see Figs. 6 and 7). For rF45-R627C, trypsin- and chymotrypsin-sensitive sites were identified in the last loop of the cbEGF module 6 between C5 and C6, relatively close to the mutated residue. These results demonstrate that the additional cysteine at position 627 causes short range structural changes in the loop attacked by proteases. No sensitive sites have been found in the preceding cbEGF module 5 or the following 8-Cys/TB module 2. For rF45-C750G, cleavage sites have been found in the loops between C3 and C4 and between the (mutated) C5 and C6 of cbEGF module 7, demonstrating short range structural effects introduced by C750G. Additionally, sensitive sites between C1 and C2 and between C3 and C4 of the following cbEGF module 8 indicated long range structural effects transmitted to the next cbEGF module. Two subsequent cbEGF modules are stabilized by calcium ligation and,

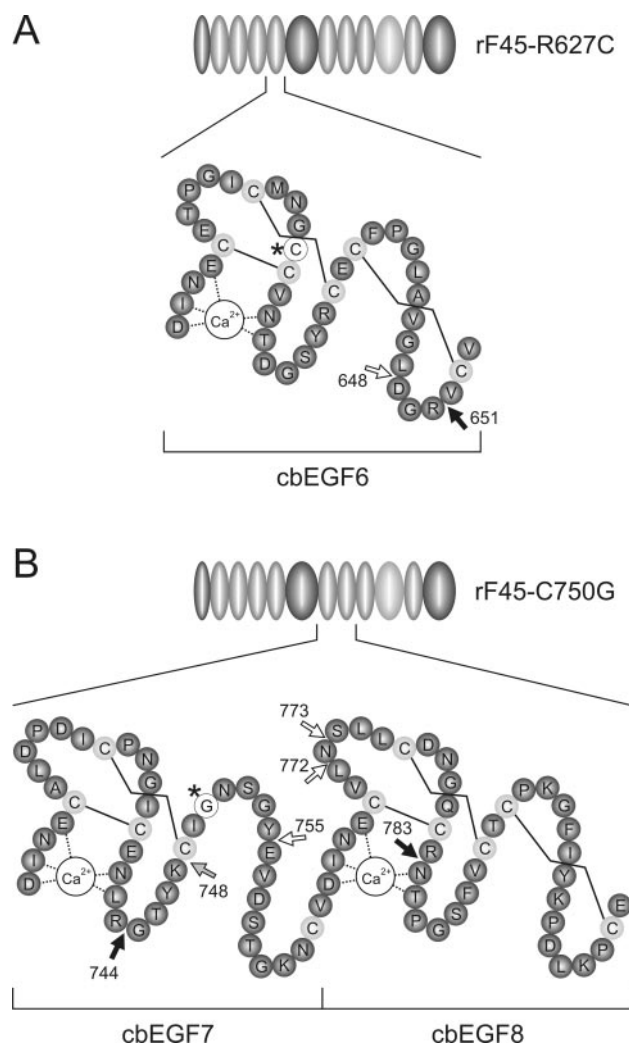


FIG. 7. Localization of proteolytic sites rendered susceptible by mutations R627C (A) and C750G (B). The upper parts of each image show the entire recombinant polypeptide, and the lower parts show the cbEGF modules, which contain the mutations (\*) and the proteolytic sites identified. Amino acid residues are represented by circles, and disulfide bonds are shown by lines. The sensitive sites (see Fig. 6 and Table II) produced by chymotrypsin (white arrows), trypsin (black arrows), and plasmin (gray arrows) are mapped, and the position C-terminal to the cut site is indicated for each site.

additionally, by interdomain hydrophobic packing interaction involving a conserved aromatic residue at the open end of the minor  $\beta$ -sheet (between C5 and C6) of the preceding cbEGF module and the top of the major  $\beta$ -sheet (between C3 and C4) of the following cbEGF module (9, 38). It is likely that the replacement of the cysteine residue in the C5 position of cbEGF module 7 by a glycine residue, which prevents formation of the C5-C6 disulfide bond, destabilizes the minor  $\beta$ -sheet of cbEGF module 7. This may in turn further destabilize the hydrophobic interdomain interactions and expose the loop between the cysteines at the C3 and C4 positions of cbEGF module 8 to proteases. Subsequently or concomitantly, the loop between cysteines at the C1 and C2 positions of cbEGF module 8, which is not involved in interdomain stabilization, also becomes destabilized and susceptible to proteolytic attack. Whereas chymotrypsin and trypsin are used as biochemical tools, plasmin may be a protease of physiological significance, since it is available in extracellular matrices at sites where fibrillin-1 and microfibrils are expressed (39).

For rF45-C926R, we obtained indirect evidence for enhanced proteolytic susceptibility. In Western blot analyses, the se-

creted product appeared smaller than expected, indicating proteolytic cleavage close to the C-terminal end of the polypeptide in close vicinity of the mutation in cbEGF module 10 (see Fig. 1A). In addition, as stated above, the fact that it was not possible to purify sufficient amounts of rF45-C926R may indicate proteolytic degradation during the purification procedure. Clearly, more detailed studies about potential physiological proteases involved in degradation processes must follow.

On the molecular level, it is not clear how the plethora of mutations in cbEGF modules all can lead to variable but yet similar clinical phenotypes. On the cell culture level with isolated fibroblasts from individuals with MFS, defects have been characterized affecting synthesis, secretion, and matrix deposition of fibrillin-1 (24, 40, 41). These mechanisms are predicted to lead to less functional microfibrils in tissues. Enhanced proteolytic susceptibility could explain the deleterious effects of mutations on several levels; if the protein becomes degraded as a monomer in the secretory pathway or early in the extracellular compartment, then consequently less fibrillin-1 would be available for incorporation into microfibrils. If mutated fibrillin-1 becomes degraded in assembled microfibrils, then this may lead to "weakened" microfibrils, which may lose their full functional spectrum over time. Enhanced proteolytic degradation of recombinant mutation constructs has been observed as the consequence for a number of noncysteine mutations such as N548I, E1073K, K1300E, D1406G, N2183S, and E2447K (20–23, 26). The results presented here, together with the data by Booms *et al.* (26) demonstrating enhanced susceptibility for a cysteine mutation at the C6 position (C1320S), significantly expand this concept to the large group of cysteine mutations leading to MFS and other fibrillinopathies. For some mutations analyzed on the molecular level such as E2169K or N2144S, no enhanced susceptibility to proteolysis has been observed (21, 23). However, only a few proteases have been tested with these constructs, leaving the possibility open that other proteases may be able to attack these mutated polypeptides. Whether or not the biochemical phenotype of a given missense mutation is indeed "enhanced proteolytic susceptibility" depends (i) on the availability of recognition sites in the protein, (ii) on the exposure of these sites induced by the mutation, and (iii) on the presence of active proteases that are able to recognize these sites in a physiological context. Identification of such candidate proteases will therefore be an important next step.

**Acknowledgments**—We thank Rainer Bartels for N-terminal sequencing; Karin Wiessmann for electron microscopy; and Martina Alexander, Katja Thiele, and Stefanie Schulz for outstanding technical assistance. We are grateful to Lynn Y. Sakai and the staff of the Sakai laboratory for providing the mAb 201 antibody and for consistent help.

#### REFERENCES

- Sakai, L. Y., Keene, D. R., and Engvall, E. (1986) *J. Cell Biol.* **103**, 2499–2509
- Zhang, H., Apfelroth, S. D., Hu, W., Davis, E. C., Sanguineti, C., Bonadio, J., Mecham, R. P., and Ramirez, F. (1994) *J. Cell Biol.* **124**, 855–863
- Maslen, C. L., Corson, G. M., Maddox, B. K., Glanville, R. W., and Sakai, L. Y. (1991) *Nature* **352**, 334–337
- Lee, B., Godfrey, M., Vitale, E., Hori, H., Mattei, M. G., Sarfarazi, M., Tsipouras, P., Ramirez, F., and Hollister, D. W. (1991) *Nature* **352**, 330–334
- Corson, G. M., Chalberg, S. C., Dietz, H. C., Charbonneau, N. L., and Sakai, L. Y. (1993) *Genomics* **17**, 476–484
- Pereira, L., D'Alessio, M., Ramirez, F., Lynch, J. R., Sykes, B., Pangilinan, T., and Bonadio, J. (1993) *Hum. Mol. Genet.* **2**, 961–968
- Corson, G. M., Charbonneau, N. L., Keene, D. R., and Sakai, L. Y. (2004) *Genomics* **83**, 461–472
- Campbell, I. D., and Bork, P. (1993) *Curr. Opin. Struct. Biol.* **3**, 385–392
- Downing, A. K., Knott, V., Werner, J. M., Cardy, C. M., Campbell, I. D., and Handford, P. A. (1996) *Cell* **85**, 597–605
- Reinhardt, D. P., Ono, R. N., and Sakai, L. Y. (1997) *J. Biol. Chem.* **272**, 1231–1236
- Reinhardt, D. P., Mechling, D. E., Boswell, B. A., Keene, D. R., Sakai, L. Y., and Bächinger, H. P. (1997) *J. Biol. Chem.* **272**, 7368–7373
- Saharinen, J., Hyytiäinen, M., Taipale, J., and Keski-Oja, J. (1999) *Cytokine Growth Factor Rev.* **10**, 99–117
- Milewicz, D. M., Urban, Z., and Boyd, C. (2000) *Matrix Biol.* **19**, 471–480
- Colod-Beroud, G., Le Bourdelles, S., Ades, L., Ala-Kokko, L., Booms, P., Boxer, M., Child, A., Comeglio, P., De Paepe, A., Hyland, J. C., Holman, K., Kaitila, I., Loays, B., Matyas, G., Nuytink, L., Peltonen, L., Rantamaki, T., Robinson, P., Steinmann, B., Junien, C., Beroud, C., and Boileau, C. (2003) *Hum. Mutat.* **22**, 199–208
- Pyeritz, R. E. (2000) *Annu. Rev. Med.* **51**, 481–510
- Dietz, H. C., McIntosh, I., Sakai, L. Y., Corson, G. M., Chalberg, S. C., Pyeritz, R. E., and Francomano, C. A. (1993) *Genomics* **17**, 468–475
- Hewett, D., Lynch, J., Child, A., Firth, H., and Sykes, B. (1994) *Am. J. Hum. Genet.* **55**, 447–452
- Halliday, D., Hutchinson, S., Kettle, S., Firth, H., Wordsworth, P., and Handford, P. A. (1999) *Hum. Genet.* **105**, 587–597
- Montgomery, R. A., Geraghty, M. T., Bull, E., Gelb, B. D., Johnson, M., McIntosh, I., Francomano, C. A., and Dietz, H. C. (1998) *Am. J. Hum. Genet.* **63**, 1703–1711
- Robinson, P. N., and Booms, P. (2001) *Cell. Mol. Life Sci.* **58**, 1698–1707
- Ashworth, J. L., Murphy, G., Rock, M. J., Sherratt, M. J., Shapiro, S. D., Shuttleworth, C. A., and Kielty, C. M. (1999) *Biochem. J.* **340**, 171–181
- Reinhardt, D. P., Ono, R. N., Notbohm, H., Müller, P. K., Bächinger, H. P., and Sakai, L. Y. (2000) *J. Biol. Chem.* **275**, 12339–12345
- McGettrick, A. J., Knott, V., Willis, A., and Handford, P. A. (2000) *Hum. Mol. Genet.* **9**, 1987–1994
- Schrijver, I., Liu, W., Brenn, T., Furthmayr, H., and Francke, U. (1999) *Am. J. Hum. Genet.* **65**, 1007–1020
- Whiteman, P., and Handford, P. A. (2003) *Hum. Mol. Genet.* **12**, 727–737
- Booms, P., Tietze, F., Rosenberg, T., Hagemeier, C., and Robinson, P. N. (2000) *Hum. Genet.* **107**, 216–224
- Hayward, C., Rae, A. L., Porteous, M. E., Logie, L. J., and Brock, D. J. (1994) *Hum. Mol. Genet.* **3**, 373–375
- Nijbroek, G., Sood, S., McIntosh, I., Francomano, C. A., Bull, E., Pereira, L., Ramirez, F., Pyeritz, R. E., and Dietz, H. C. (1995) *Am. J. Hum. Genet.* **57**, 8–21
- Jensen, S. A., Reinhardt, D. P., Gibson, M. A., and Weiss, A. S. (2001) *J. Biol. Chem.* **276**, 39661–39666
- Reinhardt, D. P., Keene, D. R., Corson, G. M., Pöschl, E., Bächinger, H. P., Gambee, J. E., and Sakai, L. Y. (1996) *J. Mol. Biol.* **258**, 104–116
- Chen, C., and Okayama, H. (1987) *Mol. Cell. Biol.* **7**, 2745–2752
- Lin, G., Tiedemann, K., Vollbrandt, T., Peters, H., Bätge, B., Brinckmann, J., and Reinhardt, D. P. (2002) *J. Biol. Chem.* **277**, 50795–50804
- Keene, D. R., Jordan, C. D., Reinhardt, D. P., Ridgway, C. C., Ono, R. N., Corson, G. M., Fairhurst, M., Sussman, M. D., Memoli, V. A., and Sakai, L. Y. (1997) *J. Histochem. Cytochem.* **45**, 1069–1082
- Reinhardt, D. P., Sasaki, T., Dzamba, B. J., Keene, D. R., Chu, M. L., Göhring, W., Timpl, R., and Sakai, L. Y. (1996) *J. Biol. Chem.* **271**, 19489–19496
- Booms, P., Cislis, J., Mathews, K. R., Godfrey, M., Tietze, F., Kaufmann, U. C., Vetter, U., Hagemeier, C., and Robinson, P. N. (1999) *Clin. Genet.* **55**, 110–117
- Adam, S., Goehring, W., Wiedemann, H., Chu, M. L., Timpl, R., and Kostka, G. (1997) *J. Mol. Biol.* **272**, 226–236
- Whiteman, P., Smallridge, R. S., Knott, V., Cordle, J. J., Downing, A. K., and Handford, P. A. (2001) *J. Biol. Chem.* **276**, 17156–17162
- Smallridge, R. S., Whiteman, P., Werner, J. M., Campbell, I. D., Handford, P. A., and Downing, A. K. (2003) *J. Biol. Chem.* **279**, 12199–12206
- Mignatti, P., and Rifkin, D. B. (1996) *Enzyme Protein* **49**, 117–137
- Milewicz, D., Pyeritz, R. E., Crawford, E. S., and Byers, P. H. (1992) *J. Clin. Invest.* **89**, 79–86
- Aoyama, T., Franke, U., Dietz, H. C., and Furthmayr, H. (1994) *J. Clin. Invest.* **94**, 130–137

## **Consequences of Cysteine Mutations in Calcium-binding Epidermal Growth Factor Modules of Fibrillin-1**

Tillman Vollbrandt, Kerstin Tiedemann, Ehab El-Hallous, Guoqing Lin, Jürgen Brinckmann, Harald John, Boris Bätge, Holger Notbohm and Dieter P. Reinhardt

*J. Biol. Chem.* 2004, 279:32924-32931.

doi: 10.1074/jbc.M405239200 originally published online May 25, 2004

---

Access the most updated version of this article at doi: [10.1074/jbc.M405239200](https://doi.org/10.1074/jbc.M405239200)

Alerts:

- [When this article is cited](#)
- [When a correction for this article is posted](#)

[Click here](#) to choose from all of JBC's e-mail alerts

This article cites 38 references, 10 of which can be accessed free at <http://www.jbc.org/content/279/31/32924.full.html#ref-list-1>